Available online at www.sciencedirect.com
ScienceDirect
Materials Chemistry and Physics 101 (2007) 170–176
MATERIALS CHEMISTRY AND PHYSICS
www.elsevier.com/locate/matchemphys

Effect of substituents on the photoluminescent and electroluminescent properties of substituted cyclometalated iridium(III) complexes

Hsiao-Wen Hong, Teng-Ming Chen *

Department of Applied Chemistry, National Chiao Tung University, Hsinchu 30055, Taiwan

Received 20 October 2005; received in revised form 10 February 2006; accepted 22 March 2006

Abstract

The photophysics of octahedral $4d^6$ and $5d^6$ complexes has been studied extensively. The d^6 iridium(III) complexes show intense phosphorescence at room temperature. Our goal of this research is to study the synthesis, characterization and applications of the light emitting dopants based on iridium(III) complexes. We have prepared and characterized a series of substituted (4-CF_3, 4-Me, 4-OMe, 4-F, 3-F) 2-phenylbenzoxazole ligand. The intermediate di-irrido and the six-coordinated mononuclear iridium(III) dopants of the above ligands have been synthesized and characterized. These complexes are thermally stable between 280–320 °C depending upon the substituents and sublimable. They emit bright yellow to green light. The peak emission wavelengths of the dopants can be finely tuned depending upon the electronic properties of the substituents as well as their positions in the ring. The emission spectral diagrams show that the emissive states of the complexes have major contribution of MLCT state. In the absorption spectra, the ^{1}MLCT and ^{3}MLCT transitions have been resolved in the range, 385–500 nm. The physical parameters of the electroluminescent devices for the substituted and the unsubstituted complexes has been compared and discussed.

Keywords: Photoluminescence; Electroluminescence; OLED; Ir complexes

1. Introduction

A significant research effort has been focused on the synthesis and photophysical characterization of octahedral $4d^6$ and $5d^6$ metal complexes. Luminescent d^6 metal complexes of Re(I), Ru(II), Os(II) and Ir(III) have attracted considerable attention due to their intriguing photophysical, photochemical and excited state redox properties [1] and potential applications in photonic and photoelectronic devices [2]. Strong spin–orbit coupling of the 4d or 5d ion leads to efficient intersystem crossing of the singlet excited states to the triplet manifold. More recently, a number of groups have investigated the Rh^{3+} and Ir^{3+} metal complexes and there also have been growing interests in electroluminescent devices (EL) with phosphor complex dopants of the above metals as emitting layers [3–6]. The research group lead by Mark Thompson et al. have synthesized and reported a series of neutral emissive cyclometalated complexes of iridium(III) [7] and platinum(II) [8] and used them in the fabrication of organic light emitting diode (OLEDs) as a phosphorescent dopant successively. Researchers from Dupont de Nemours and Co. have also synthesized and characterized a series of iridium(III) complexes with fluorinated 2-arylpyridines and showed that the emissive colors of the materials can be finely tuned by systematic control of the nature and position of the substituents of the ligands [9]. These research activities inspired us to initiate a systematic study to investigate the color tuning of the iridium(III) complexes by choosing a particular cyclometalated ligand with substituents exhibiting different electronic properties. Of the above phosphor emitters that have been reported for (OLED) devices, iridium(III)-based materials have displayed the most promising due to their high stability, high photoluminescence (PL) efficiency and relatively short excited state lifetime. So, we choose 2-phenylbenzoxazole (bo) as the cyclometalated ligand with substituents (i.e., -CF_3, -F, -Me, -OMe) showing different electronic properties to synthesize mononuclear emissive complex with iridium(III). We present the syntheses and photophysical studies of (x/ybo)$_2$Ir(acac) (x = 4-CF_3, 4-F, 4-Me, 4-OMe; y = 3-F; acac = acetylacetonate) and their applications in OLEDs.

* Corresponding author. Fax: +886 35723764.
E-mail address: tmchen@mail.nctu.edu.tw (T.-M. Chen).

0254-0584/$ – see front matter © 2006 Elsevier B.V. All rights reserved.
doi:10.1016/j.matchemphys.2006.03.011

2. Experimental section

2.1. Materials

All of the preparative work involving iridium(III) trichloride hydrate ($IrCl_3 \cdot 3H_2O$, Alfa Aesar Company Ltd.), 2-ethoxyethanol ($H_5C_2OC_2H_4OH$, Fluka) and all other reagents (Tokyo Chemical Industry, Japan) were carried out in inert atmosphere and used without further purification.

2.2. Optical measurements and compositions analysis

The ultraviolet–visible (UV–vis) spectra of the phosphorescent Ir(III) complexes were measured on an UV–vis spectrophotometer (Agilent model 8453) and corrected for background due to solvent absorption. Photoluminescence (PL) spectra were carried out with a spectrophotometer (Jobin-Yvon Spex, model Fluorolog-3). Solution photoluminescence quantum efficiency were measured by a relative method [22] using $Ir(ppy)_3$ [21] as standard in dichloromethane. NMR spectra were recorded on Varian 300 MHz and MS spectra (both EI and FAB) were taken on an Micromass TRIO-2000. Cyclic voltammetry (CV) analyses were performed by using CHI 2.05, the TG–DTA analysis was carried out by using a thermal analyzer (SEIKO 1TG/DTA 200).

2.2.1. Synthesis of x/y(bo) (x = 4-CF_3, 4-F, 4-Me, 4-OMe and y = 3F; bo = 2-phenylbenzoxazole) and complexes with unsubstituted ligands

Synthesis of x/y(bo) (x = 4-CF_3, 4-F, 4-Me, 4-OMe and y = 3-F; bo = (2-phenyl)benzoxazole): these were prepared by a general method [10] where 10 mmol *o*-aminophenol was dissolved into 20 ml of 1-methyl-pyrrolidinone under inert atmosphere; then the stoichiometric amount of the corresponding acid chloride was added slowly at room temperature. The mixture was heated at 100 °C for 1 h. After cooling, the solution was poured into cold water and the mixture was adjusted to pH 8–9 with 7N aqueous ammonia. A white colored solid compound was separated out. The crude material was filtered, washed with water for several times and then purified by column chromatography.

bo: 2-phenylbenzoxazole. ^{1}H NMR (300 MHz, $CDCl_3$): 7.86 (m, 3H), 7.64 (d, 8.1, 1H), 7.25 (m, 4H), 7.13 (m, 1H), EIMS: *m/z* 195, Calcd. 195.

(4-MeO)bo: (4-methoxy)2-phenylbenzoxazole. ^{1}H NMR (300 MHz, $CDCl_3$): 8.22 (d, 2H, *J* 1.5 Hz), 7.74 (m, 1H), 7.56 (m, 1H), 7.31 (m, 2H), 3.90 (s, 3H), EIMS: *m/z* 225, Calcd. 225.

(4-CF_3)bo: (4-trifluoromethyl)2-phenylbenzoxazole. ^{1}H NMR (300 MHz, $CDCl_3$): δ, ppm 8.38 (d, 2H, *J* 8.1 Hz), 8.11 (d, 3H, *J* 3.3 Hz), 7.61 (m, 1H), 7.44 (m, 2H), EIMS: *m/z*: 263, Calcd. 263.

(4-Me)bo: (4-methyl)2-phenylbenzoxazole. ^{1}H NMR (300 MHz, $CDCl_3$): δ, ppm 8.05 (d, 1H, *J* 8.4 Hz), 7.98 (d, 2H, *J* 8.4 Hz), 7.88 (dd, 1H, *J* 0.6, 8.1 Hz), 7.47 (t, 1H, *J* 7.5 Hz), 7.36 (t, 1H, *J* 7.2 Hz), 7.27 (d, 2H, *J* 7.8 Hz), EIMS: *m/z*: 209, Calcd. 209.

(4-F)bo: (4-fluoro)2-phenylbenzoxazole. ^{1}H NMR (300 MHz, $CDCl_3$): δ, ppm 8.35 (s, 1H), 7.93 (m, 1H), 7.90 (m, 2H), 7.14 (m, 2H), 7.05 (d, 1H, *J* 8.1 Hz), 6.91 (t, 1H, *J* 6.6, 6.9 Hz), EIMS: *m/z*: 213, Calcd. 213.

(3-F)bo: (3-fluoro)2-phenylbenzoxazole. ^{1}H NMR (300 MHz, $CDCl_3$): δ, ppm 8.21 (s, 1H), 7.66 (m, 2H), 7.52 (m, 2H), 7.17 (d, 1H, *J* 8.7), 7.07 (d, 1H, *J* 8.1 Hz), 6.95 (t, 1H, *J* 6.3, 6.9 Hz), EIMS: *m/z*: 213, Calcd. 213.

2.2.2. Synthesis of dinuclear iridium(III) complexes, x/y(bo)$_2$Ir(μ-Cl)$_2$x/y(bo)$_2$

Synthesis of the dichoro-bridged iridium(III) complexes, x/ybo$_2$Ir(μ-Cl)$_2$x/ybo$_2$: these were prepared by refluxing the mixture of $IrCl_3$ (1 mmol) and the ligands (x/ybo) (2.4 mmol) in 2-ethoxyethanol for 24–25 h. The orange-yellow mixture was cooled to room temperature and 20 ml 1 M HCl was added to precipitate the product. The mixture was filtered and washed with 100 ml 1 M HCl followed by 50 ml methanol solution for several times then dried.

[Ir(bo)$_2$Cl$_2$]$_2$: ^{1}H NMR (300 MHz, $CDCl_3$): δ, ppm 8.23 (d, 4H, *J* 7.8 Hz), 7.56 (d, 4H, *J* 7.5 Hz), 7.16 (d, 4H, *J* 7.2 Hz), 6.96 (d, 4H, *J* 7.5 Hz), 6.72 (d, 4H, *J* 7.2 Hz), 6.05 (s, 4H), 1.98 (s, 12H), FABMS: *m/z* 1232, Calcd. 1232.

[Ir(4-MeObo)$_2$Cl$_2$]$_2$: ^{1}H NMR (300 MHz, $CDCl_3$): δ, ppm 8.14 (d, 4H, *J* 7.8 Hz), 7.55 (d, 4H, *J* 8.4, 2.4 Hz), 7.25 (d, 4H, *J* 9.0 Hz), 7.00 (t, 4H, *J* 7.5, 8.4 Hz), 6.86 (t, 4H, *J* 8.1, 7.2 Hz), 6.44 (d, 4H, *J* 8.7 Hz), 5.71 (s, 4H), 3.25 (s, 12H), FABMS: *m/z* 1351, Calcd. 1351.

[Ir(4-CF$_3$bo)$_2$Cl$_2$]$_2$: ^{1}H NMR (300 MHz, $CDCl_3$): δ, ppm 8.12 (d, 4H, *J* 7.2 Hz), 7.76 (d, 4H, *J* 8.1 Hz), 7.41 (d, 4H, *J* 8.4 Hz), 7.29 (d, 4H, *J* 0.06 Hz), 7.16 (d, 4H, *J* 7.8 Hz), 7.01 (t, 4H, *J* 8.4, 8.1 Hz), 6.38 (s, 4H), FABMS: *m/z* 1504, Calcd. 1504.

[Ir(4-Mebo)$_2$Cl$_2$]$_2$: ^{1}H NMR (300 MHz, $CDCl_3$): δ, ppm 8.23 (d, 4H, *J* 7.8 Hz), 7.56 (d, 4H, *J* 7.5 Hz), 7.16 (d, 4H, *J* 7.2 Hz), 6.96 (d, 4H, *J* 7.5 Hz), 6.72 (d, 4H, *J* 7.2 Hz), 6.05 (s, 4H), 1.98 (s, 12H), FABMS: *m/z* 1287, Calcd. 1287.

[Ir(4-Fbo)$_2$Cl$_2$]$_2$: ^{1}H NMR (300 MHz, $CDCl_3$): δ, ppm 8.16 (d, 4H, *J* 8.1 Hz), 7.69 (dd, 4H, *J* 5.7, 7.8 Hz), 7.35 (d, 4H, *J* 8.1 Hz), 7.17 (t, 4H, *J* 8.4, 7.8 Hz), 6.96 (t, 4H, *J* 8.1, 7.5 Hz), 6.67 (t, 4H, *J* 8.7, 8.6 Hz), 5.82 (dd, 4H, *J* 9.9, 1.2 Hz), FABMS: *m/z* 1303, Calcd. 1303.

[Ir(3-Fbo)$_2$Cl$_2$]$_2$: ^{1}H NMR (300 MHz, $CDCl_3$): δ, ppm 8.33 (d, 4H, *J* 8.1 Hz), 7.63 (d, 4H, *J* 6.6 Hz), 7.20 (m, 8H), 7.02 (m, 8H), 6.37 (s, 4H), FABMS: *m/z* 1303, Calcd. 1303.

2.2.3. Syntheses of mononuclear iridium(III) complex dopants (x/ybo)$_2$Ir(acac)

The chloride bridged dinuclear iridium(III) complex (x/ybo)$_2$Ir(μ-Cl)$_2$Ir(x/ybo)$_2$ (0.1 mmol), acetylacetone (0.3 mmol) and sodium carbonate (1 mmol) were mixed in 10 ml of 2-ethoxyethanol (30 ml). The mixture was refluxed under nitrogen for 11–12 h. The reaction mixture was then cooled and the resulted precipitate was collected through filtration. The product was purified by recrystallization from a solution of the mixture of dichloromethane and methanol (2:1).

Ir(bo)$_2$(acac): ^{1}H NMR (300 MHz, $CDCl_3$): δ, ppm 8.25 (d, 2H), 7.93 (m, 2H), 7.74 (dd, 2H, *J* 8.1, 1.9 Hz), 7.56 (m, 4H), 6.86 (td, 2H, *J* 7.8, 1.1 Hz), 6.59 (td, 2H, *J* 7.5, 1.0 Hz), 6.2 (d, 2H, *J* 7.5 Hz), 5.12 (s, 1H), 1.71 (s, 6H), FABMS: *m/z* 680, Calcd. 680.

Ir(4-MeObo)$_2$(acac): ^{1}H NMR (300 MHz, $CDCl_3$): δ, ppm 7.59 (d, 4H, *J* 8.4 Hz), 7.47 (m, 2H), 7.34 (m, 4H), 6.45 (dd, 2H, *J* 8.4, 2.4 Hz), 5.98 (s, 2H), 5.22 (s, 2H), 3.47 (s, 6H), 1.82 (s, 6H), FABMS: *m/z* 741, Calcd. 741.

Ir(4-CF$_3$bo)$_2$(acac): ^{1}H NMR (300 MHz, $CDCl_3$): δ, ppm 7.74 (t, 4H, *J* 8.1, 7.8 Hz), 7.51 (t, 4H, *J* 6.9, 7.2 Hz), 7.43 (d, 2H, *J* 8.1 Hz), 7.13 (d, 2H, *J* 8.7 Hz), 6.64 (s, 2H), 5.24 (s, 1H), 1.83 (s, 6H), FABMS: *m/z* 816, Calcd. 816.

Ir(4-Mebo)$_2$(acac): ^{1}H NMR (300 MHz, $CDCl_3$): δ, ppm 7.64 (d, 2H, *J* 6.9 Hz), 7.51 (m, 4H), 7.36 (m, 4H), 6.67 (d, 2H, *J* 7.2 Hz), 6.29 (s, 2H), 1.95 (s, 6H), 1.81 (s, 6H), FABMS: *m/z* 708, Calcd. 708.

Ir(4-Fbo)$_2$(acac): ^{1}H NMR (300 MHz, $CDCl_3$): δ, ppm 7.65 (t, 4H, *J* 8.7, 5.7 Hz), 7.43 (m, 6H), 6.60 (m, 2H), 6.09 (d, 2H, *J* 9.9 Hz), 5.26 (s, 1H), 1.83 (s, 6H), FABMS: *m/z* 716, Calcd. 716.

Ir(3-Fbo)$_2$(acac): ^{1}H NMR (300 MHz, $CDCl_3$): δ, ppm 7.65 (d, 2H, *J* 7.8 Hz), 7.54 (m, 4H), 7.41 (m, 4H), 6.91 (m, 2H), 6.39 (t, 2H, *J* 8.4, 8.4 Hz), 5.30 (s, 2H), 1.86 (s, 6H), FABMS: *m/z* 716, Calcd. 716.

2.3. Crystallography

Diffraction data for (CF$_3$bo)$_2$Ir(acac) single crystals were collected on a Bruker CCD diffractometer with Mo Kα (λ = 0.71073 Å). Data collection in the 2θ scan mode, cell refinement and data reduction were carried out using program Bruker SHELXTL. The structure was solved by direct methods using the SHELXS-97 package of computer programs. The structure was refined by full-matrix least-squares methods based on F^2 using SHELXL-97. The non-hydrogen atom positions were refined anisotropically whereas the hydrogen positions were not refined.

2.4. OLED fabrication and testing

Organic layers were fabricated by high-vacuum thermal evaporation onto a glass substrate precoated with an indium–tin–oxide (ITO) layer with a sheet resistance of 20 Ω. Prior to use, the ITO surface was ultrasonicated in a detergent solution followed by rinsing with deionized (DI) water, dipped into acetone, trichloroethylene, and 2-propanol, and then degreased with a vapor of 2-propanol. After degreasing, the substrate was oxidized and cleaned in a UV-ozone chamber before it was loaded into an evaporator. In a vacuum chamber at pressure of 10^{-6} Torr, 500 Å of NPB as the hole transporting layer; 200 Å the complex doped (7%) CBP as the emitting layer; 100 Å of 2,9-dimethyl-

4,7-diphenyl-1, 10-phenanthroline (BCP) as a hole and exciton blocking layer (HBL); 650 Å of Alq_3 as electron transport layer; and a cathode composed of 10 Å lithium fluoride and 2000 Å aluminum were sequentially deposited onto the substrate to give the device structure. The current–voltage (*I–V*) profiles and light intensity characteristics for the above-fabricated devices were measured in a vacuum chamber of 10^{-6} Torr at ambient temperature using a Keithley 2400 Source Meter/2000 Multimeter coupled to a PR 650 Optical Meter.

3. Results and discussion

3.1. Synthesis and characterization of $(x/ybo)_2Ir(acac)$ complexes

Iridium complexes were prepared according to the procedure reported previously [11]. The synthesis of the ligands and iridium complexes is depicted in Eq. (1). Complexes of $(x/ybo)_2Ir(acac)$ have been prepared [7] with all the substituents in the cyclometalated ligand bo. The synthetic method used to prepare these complexes involves two steps. In the first step, $IrCl_3{\cdot}3H_2O$ is allowed to react with an excess of the cyclometalated ligand (2.5 times) to give a chloro-bridged dinuclear complex, i.e. $(x/ybo)_2Ir(\mu\text{-}Cl)_2Ir(x/ybo)_2$.

$$2IrCl_3{\cdot}3H_2O + 4\,(x/ybo) \rightarrow (x/ybo)_2Ir(\mu\text{-}Cl)_2Ir(x/ybo)_2 + 4HCl + 3H_2O(g) \quad (1)$$

$$(x/ybo)_2Ir(\mu\text{-}Cl)_2Ir(x/ybo)_2 + 2L\text{^}XH \rightarrow 2(x/ybo)_2Ir(L\text{^}X) + 2HCl \quad (2)$$

The chloro-bridged dinuclear complexes can be readily converted to emissive, mononuclear complexes $(x/ybo)_2Ir(acac)$ by replacing the two bridging chlorides with bidentate acetylacetonate. Thus, the iridium(III) ion is octahedrally coordinated by the three chelating ligands. The coordination geometry of the "$(x/ybo)_2Ir$" fragment in the mononuclear complex is the same as that for the dinuclear complexes. All the mononuclear complex dopants with different substitutions are thermally stable up to 280–320 °C. The mononuclear Ir(III) complexes can be sublimed easily at reduced pressure.

As indicated by the reported NMR data, the resonance spectra of ligands show poorly resolved multiplets, whereas the well-resolved multiplets are observed for the complexes. The maximum high-field chemical shift is observed for the proton to the ortho-metalated carbon atom that experiences the largest shielding of any of the ligand protons. Again the chemical shift of this particular proton varies with the electronic properties of the substituents present in the ligand. The complex containing-CF_3 substituted ligand shows the lowest field chemical shift for the proton to the ortho-metalated carbon atom due to the less shielding power arising from the strong electron withdrawing property of the substituent, whereas the strongest electron-releasing substituent (i.e., $–OCH_3$ group) shows the highest field chemical shift for the same proton. The $(x/ybo)_2Ir(acac)$ complexes are stable in air and can be sublimed in a vacuum without decomposition during device fabrication.

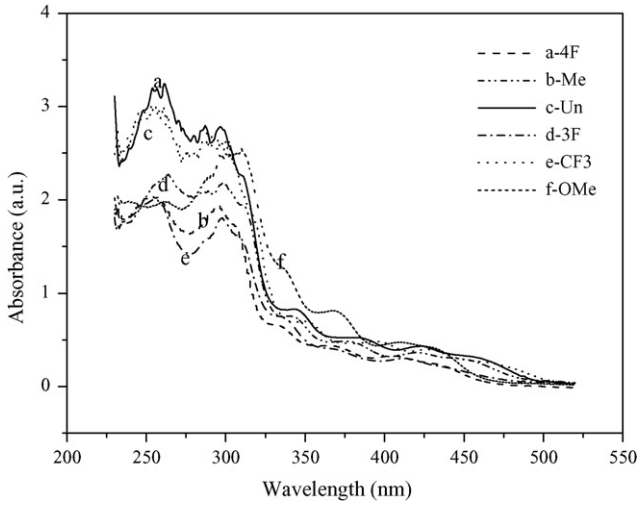

Fig. 1. Comparison of the UV–vis absorption spectra of five cyclometalled iridium complexes in CH_2Cl_2.

3.2. UV–vis absorption spectra

Fig. 1 shows the UV–visible absorption spectra for six different ligand substituted $(x/ybo)_2Ir(acac)$ complexes in CH_2Cl_2 solution at room temperature. The strong absorption bands observed at 250–300 nm are assigned to ligand centered $^1\pi$–π^* transitions, whilst the broad absorption bands at lower energy ($\lambda_{max} > 350$ nm) are typical metal to ligand charge-transfer (MLCT) transitions [12,13]. In other cyclometalated complexes these bands have been assigned to singlet and triplet MLCT transitions, and the same assignment is likely here [14]. The long tail toward lower energy is assigned to ^{3}MLCT transitions that gains intensity by mixing with the higher lying ^{1}MLCT transition through the spin–orbit coupling of iridium(III). This mixing is strong enough in these complexes that the formally spin forbidden ^{3}MLCT has an extinction coefficient that is almost equal to the spin-allowed ^{1}MLCT transition (Table 1). The presence of another transition observed at around 385 nm for the complexes is also well pronounced, which corresponds to an admixture of MLCT and ligand π–π^* states.

3.3. Photoluminescence (PL) spectra

Fig. 2 shows the PL emission spectra for $(x/y/bo)_2Ir(acac)$ complexes in CH_2Cl_2 solution at room temperature. All of these complexes show strong luminescence from the triplet states in dichloromethane solution. The emission spectra shows that all of these complexes emit in the range of 500–600 nm, which corresponds to green-yellow light. It is known that the emission bands from MLCT states are generally broad and featureless, while $^3(\pi$–$\pi^*)$ states typically give highly structured emission. It is observed that on changing the substituents in $(x/y/bo)_2Ir(acac)$ typically have effect on the maximum emission wavelength in the spectrum. Amongst all of the substituents, trifluoromethyl is the strongest electron-withdrawing group showing the emission wavelength red shift than the corresponding unsubstituted complex, $(bo)_2Ir(acac)$, and the other groups

Table 1
Spectroscopic, redox and photophysical properties for all Ir-complexes synthesized in this research

Complex (x-subs)	Absorbance, λ (nm)	Emission, λ_{max} (nm) in CH_2Cl_2	Oxidation potential versus ferrocene (volt)	HOMO (eV)[a]	LUMO (eV)	Energy gap (eV)[b]	Absolute PL efficiency[c]
Unsubstituted	386, 400	529, 562	1.036	5.317	2.837	2.48	0.4
$4CF_3$	361, 437	543, 578	1.263	5.544	3.297	2.25	0.6
4F	370, 408	511, 543	1.209	5.490	2.920	2.57	1.6
4Me	377, 430	522, 558	0.995	5.276	2.726	2.55	0.8
4OMe	362, 410	510, 543	1.013	5.294	2.754	2.54	0.1
3F	374, 418	520, 552	1.208	5.489	2.989	2.50	0.4

[a] Electrochemical properties were obtained by cyclic voltammetry using CHI 604A.
[b] The energy gap can be calculated from the edge of UV–vis absorption peak.
[c] The standard material is $Ir(ppy)_3$ in CH_2Cl_2 ($\phi = 0.4$) [21].

(F/OMe/Me) has electron-donating effects, so exhibiting the emission wavelength blue shift than the corresponding unsubstituted complex, $(bo)_2Ir(acac)$. When the position of the substitution (4F → 3F) is changed, the maximum emission wavelength (λ_{max}) of the complex shows an apparent red shifted emission [15].

The HOMO/LUMO energies have also been calculated for all the complexes and reported in Table 1 based on the experimental redox potentials and the absorption wavelengths. It is observed that the energy gap (HOMO–LUMO) for the trifluoromethyl substituted complex is the least, whereas 4-OMe and 3-F substituted complexes show the maximum energy gap and the rest exhibit intermediate values among all the investigated and these energy gap data can well be correlated with the corresponding maximum emission wavelengths of the respective complexes.

3.4. Redox chemistry

Analytical results from cyclic voltammetry indicate that all of the $(x/ybo)_2Ir(acac)$ complexes undergo a reversible one-electron oxidation; however, no reduction processes were observed in dichloromethane. The increasing order of oxidation potential of the complexes is as followings: $-CF_3 > -F > -Me > -OCH_3$ and the results are summarized in Table 1, which show the order of the strength of electron-withdrawing nature of the substituents in the complexes and, conversely, it is the increasing order of oxidation potentials.

3.5. Structure of $(CF_3bo)_2Ir(acac)$ complex

The ORTEP drawing of the $(CF_3bo)_2Ir(acac)$ complex is shown in Fig. 3. Relevant crystallographic data are given in Table 2, and selected bond lengths (Å) are presented in Table 3. These complexes have an octahedral coordination geometry around Ir and has *cis*-C,C *trans*-N,N chelate disposition. The Ir–C bonds of these complexes ($Ir–C_{av} = 2.007$ Å) are shorter than the Ir–N bonds ($Ir–N_{av} = 2.039$ Å). But the Ir–C bond length is similar to the analogues complexes reported [16]. The Ir–N bond lengths also fall within the range of values for the similar type of reported complexes. The Ir–O bond lengths of 2.110(10) and 2.124(9) Å are longer than the mean Ir–O value of 2.088 Å reported in the Cambridge Crystallographic Database [17] and reflect the large *trans* influence of the phenyl groups. All other

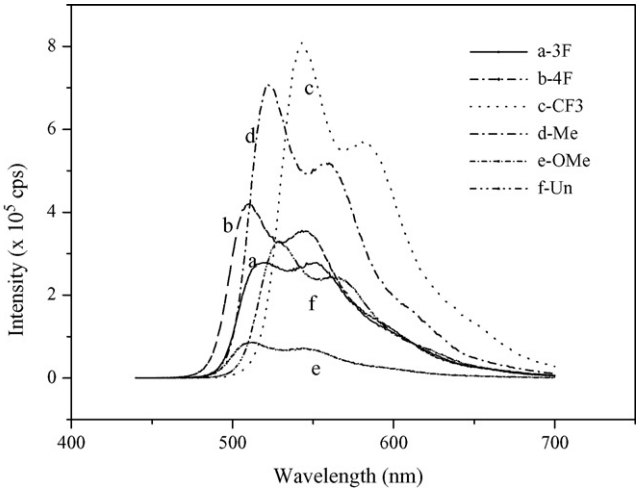

Fig. 2. Comparison of solution PL spectra for six triplet Ir(III)-based complexes in CH_2Cl_2.

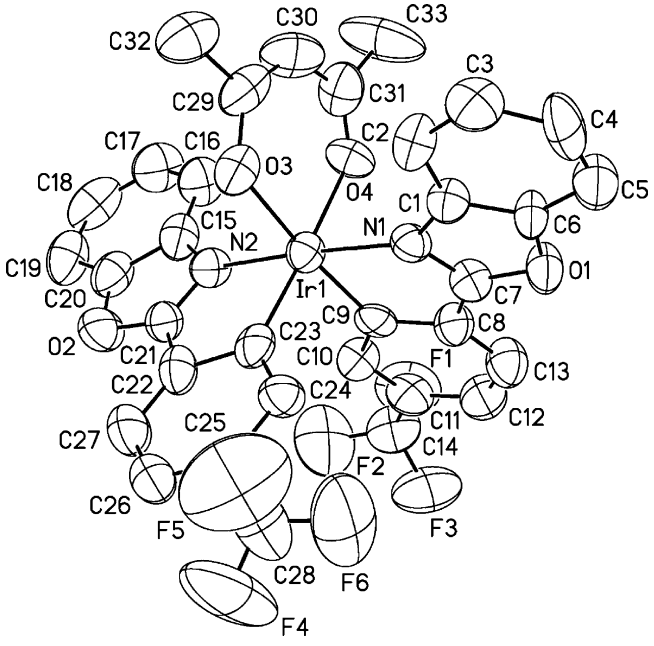

Fig. 3. ORTEP drawing of $(CF_3\text{-}bo)_2Ir(acac)$: the thermal ellipsoids represent 50% probability limit.

Table 2
Crystal data and structure refinement for $(CF_3bo)_2Ir(acac)$

Identification code	ot40 m
Empirical formula	$C_{33}H_{27}F_6IrN_2O_7$
Formula weight	869.77
Temperature	294(2) K
Wavelength	0.71073 Å
Crystal system	Monoclinic
Space group	$P2(1)/c$
Unit cell dimensions	$a = 12.211(2)$ Å (90°) $b = 20.967(4)$ Å (112.872(4)°) $c = 14.774(3)$ Å (90°)
Volume	3485.1(11) Å^3
Z	4
Density (calculated)	1.658 Mg/m^3
Absorption coefficient	3.911 mm^{-1}
$F(0\,0\,0)$	1704
Crystal size	0.20 mm × 0.08 mm × 0.05 mm
Theta range for data collection	1.78–24.73°
Index ranges	$-14 \le h \le 12$, $-24 \le k \le 24$, $-17 \le l \le 17$
Reflections collected	19584
Independent reflections	5958 (R(int) = 0.1328)
Completeness to $\theta = 24.73°$	99.8%
Absorption correction	Empirical
Maximum and minimum transmission	0.82563 and 0.45062
Refinement method	Full-matrix least-squares on F^2
Data/restraints/parameters	5958/0/442
Goodness-of-fit on F^2	0.982
Final R indices [$I > 2\sigma(I)$]	$R1 = 0.0587$, $wR2 = 0.1604$
R indices (all data)	$R1 = 0.1178$, $wR2 = 0.1768$
Largest diffraction peak and hole	1.604 and −1.132 e Å-3

Table 3
Selected bond lengths (Å) for $(CF_3\text{-}bo)_2Ir(acac)$

Atom(1)–atom(2)	Distance (Å)
Ir(1)–C(23)	2.003(15)
Ir(1)–C(9)	2.012(14)
Ir(1)–N(2)	2.029(10)
Ir(1)–N(1)	2.049(10)
Ir(1)–O(3)	2.110(10)
Ir(1)–O(4)	2.124(9)

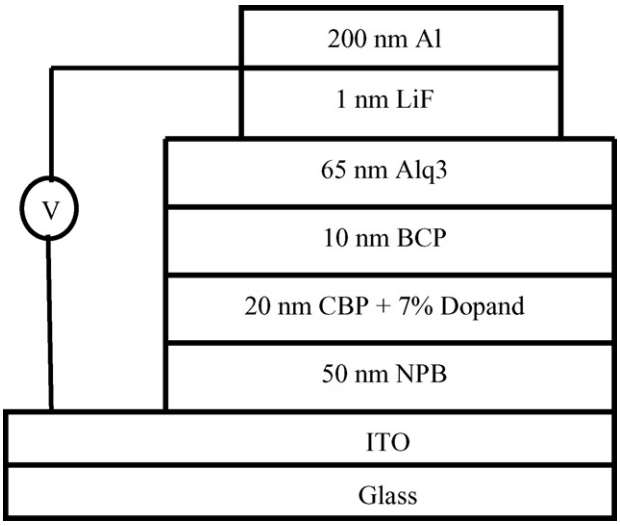

Fig. 4. EL device structures with (a) CF_3-, (b) Me-substituted (x/y-bo)$_2$Ir(acac), and (c) parent (bo)$_2$Ir(acac) complexes as a dopant.

bond lengths within the chelate ligands are analogues to the similar type of complexes reported [18–20].

3.6. Description of OLED devices fabricated with $(CF_3bo)_2Ir(acac)$, $(CH_3bo)_2Ir(acac)$ and $(bo)_2Ir(acac)$ dopants in the emissive layer

We have also fabricated three electroluminescent (EL) devices using three different iridium(III) complexes [$(CF_3bo)_2Ir(acac)$, $(CH_3bo)_2Ir(acac)$ and $(bo)_2Ir(acac)$] as dopants in the emitting layers. In order to compare the relative EL properties, we have selected two ligand substituted complex dopants [–CF_3 (device a) and –Me (device b)] with opposite electronic properties and the other is the unsubstituted bo complex (device c). These complexes were doped into the emissive layer of the OLED devices at a concentration of mole 7%. The device structure and their thickness of the layers (i.e., ITO/NPB (500 Å)/CBP + 7% dopant (200 Å)/BCP (100 Å)/Alq_3 (650 Å)/LiF (10 Å)/Al (2000 Å)) have been kept constant (Fig. 4). The comparative variation of quantum efficiency as a function of current density for these devices is shown in the Fig. 4. Furthermore, Table 4 also summarizes and compares the EL performances of devices a, b and c. It has been observed that the quantum efficiency of the devices a, b and c was found to increase with increasing current density and it

Table 4
Comparative study of the electroluminescent properties of three EL devices based on $(bo)_2Ir(acac)$, $(bo\text{-}Me)_2Ir(acac)$ an$(bo\text{-}CF_3)_2Ir(acac)$ as a dopant

	$(bo)_2Ir(acac)$	$(Me\text{-}bo)_2Ir(acac)$	$(CF_3\text{-}bo)_2Ir(acac)$
Turn-on voltage (V) at 0.5 mA/cm^2	4.62	4.64	5.33
EL color	Green	Green	Yellow
Peak wavelength (nm)	532	528	544
Luminance (cd/m^2) at 100 mA/cm^2	7546	8100	9200
Yield (cd/A) at 20 mA/cm^2	8.94	10.5	9.95
C.I.E. coordinate (x, y)	0.38, 0.56	0.37, 0.58	0.44, 0.54
Power efficiency (lm/W)	4.03 (at 4.62 V)	6.20 (at 4.64 V)	4.53 (at 5.33 V)

Device structure: ITO/NPB (500 Å)/CBP + 7% dopant (200 Å)/BCP (100 Å)/Alq3 (650 Å)/LiF (10 Å)/Al (2000 Å).

shows a maximum at 9.95, 10.5 and 8.94 cd/A at 20 mA cm^{-2}, respectively. The turn-on voltage was found to be 5.33, 4.64 and 4.62 for the devices a, b and c, respectively. The luminance efficiency was found to decrease with increasing current density for all the devices as indicated in Fig. 5 which may be attributed due to the triplet–triplet annihilation. The power efficiencies were found to be 4.53, 6.20 and 4.03 lm/W for the devices, a, b and c, respectively. At a current density 100 cd m^{-2}, the brightness of the EL device a is 9189 cd m^{-2}, whereas that for the device b and c are 8018 and 7546 cd m^{-2}, respectively. The C.I.E. was measured to be (0.44, 0.54), (0.37, 0.58) and (0.38, 0.56) for the devices, a, b and c, respectively.

The lower efficiency of the $(bo)_2Ir(acac)$ based OLED relative to that of the $(CF_3bo)_2Ir(acac)$-based device may be attributed

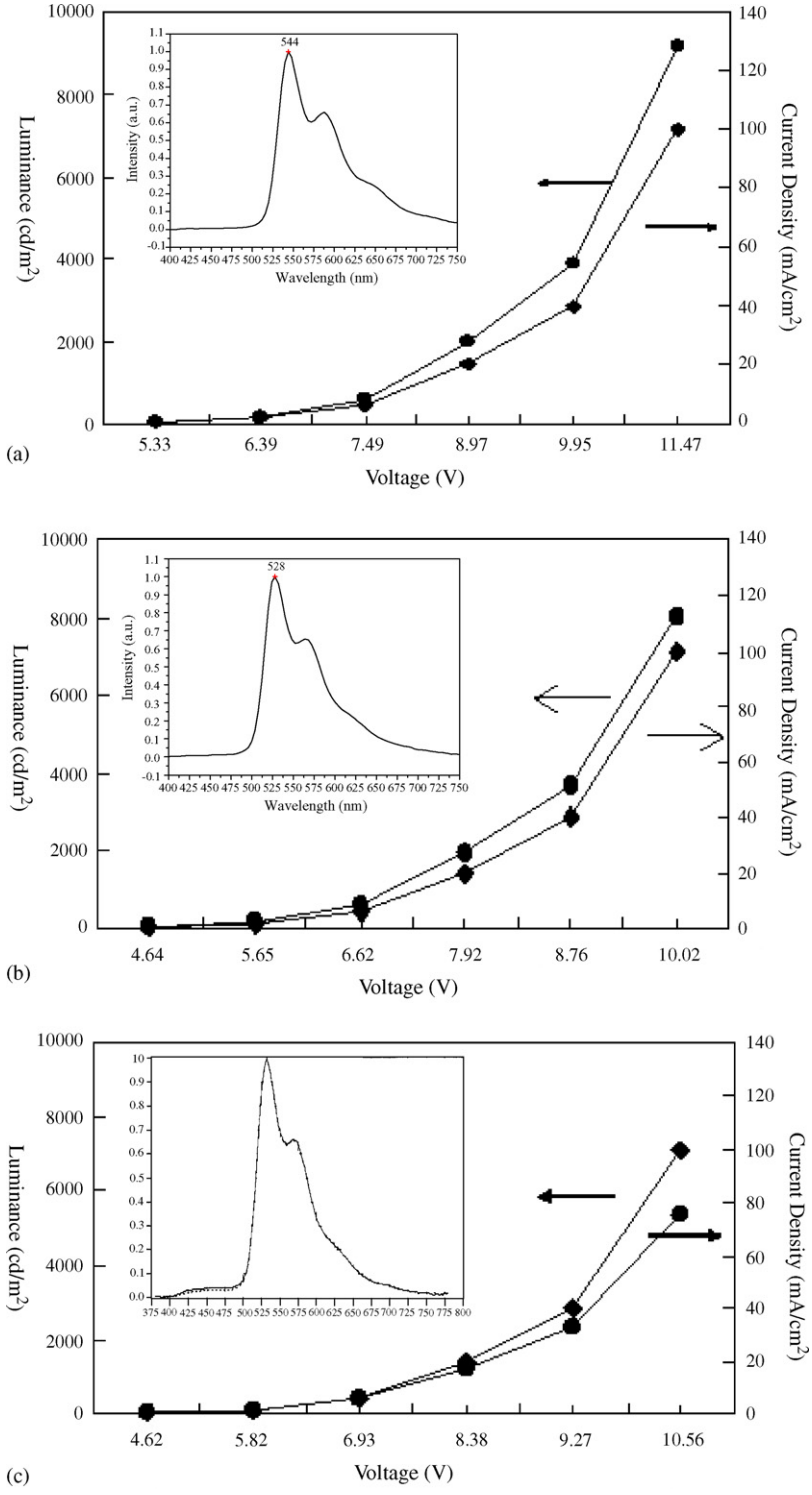

Fig. 5. EL performance of three (x/y-bo)$_2$Ir(acac) doped EL devices with x = (a) CF_3-, (b) Me-, and (c) parent $(bo)_2Ir(acac)$.

to a lower phosphorescence efficiency of the former as compared to the latter. On comparison of these devices with the corresponding devices a, b and c, power efficiency is always higher throughout the current densities and voltages applied, as indicated in Table 4, whereas the luminance and the quantum yield (described in Fig. 5) are also found to increase at lower current densities. Furthermore, no emission from CBP or Alq_3 was observed, indicating a complete energy transfer from the host exciton to the Ir-dopant. Meanwhile, there is no exciton decay in the Alq_3 layer due to the hole blocking action of the BCP layer. As shown in the insets of Fig. 5(a)–(c), the device a having trifluoromethyl-substituted dopant shows the expected red-shift and stronger intensity in the EL spectra as compared to that observed in the device c with unsubstituted dopant. Similarly, the device b having methyl-substituted dopant shows the expected blue-shift and stronger intensity in the EL spectra as compared to that observed in the device c with unsubstituted dopant. The EL spectra of a, b and c devices are similar to the PL spectra of same phosphors in a dilute solution. Thus, the EL emission is confirmed to originate from the triplet excited states of the phosphors. It is expected that the devices with the rest of the dopants synthesized and investigated in our work will exhibit more or less similar EL properties with those of devices a, b and c.

4. Conclusions

Four new cyclometallated iridium complex dopants using various types of substituted (2-phenyl)benzoxazole ligands have been synthesized and shown to exhibit high phosphorescence efficiency which made them ideal for OLED applications. These complexes show different quantum efficiencies in solution depending upon the nature of the substituents. All the complexes show one-electron oxidation in solution. The wavelength can be tuned by ca. 25 nm depending upon the electronic properties of the substituents present in the ligand. We have fabricated and investigated three EL devices and observed that the device dopants with substituted ligands show the higher luminance yield compared to the dopant with unsubstituted ligands.

Acknowledgements

This research is supported by Program for Promoting University Academic Excellence from Ministry of Education, Taiwan, Republic of China under the Contract 91-E-FA04-2-4-(B). Professor Chin Hsin Chen and OLED Laboratory of National Chiao Tung University are gratefully acknowledged for assistance with the fabrication of OLED devices and providing helpful comments on this work.

References

[1] (a) V. Balzani, A. Credi, F. Scandola, in: L. Fabbrizzi, A. Poggi (Eds.), Transition Metals in Supramolecular Chemistry, Kluwer, Dordrecht, The Netherlands, 1994, p. 1;
(b) J.-M. Lehn, Supramolecular Chemistry—Concepts and Properties, VCH, Weinheim, Germany, 1995;
(c) C.A. Bignozzi, J.R. Schoonover, F. Scandola, Prog. Inorg. Chem. 44 (1997) 1.
[2] (a) L. Tan-Sien-Hee, A.K.-D. Mesmaeker, J. Chem. Soc. Dalton Trans. 24 (1994) 3651;
(b) K.-F. Chin, K.-K. Cheung, H.-K. Yip, T.C.W. Mak, C.M. Che, J. Chem. Soc. Dalton Trans. 4 (1995) 657;
(c) K. Kalyanasundaram, M. Gratzel, Coord. Chem. Rev. 177 (1998) 347.
[3] (a) J.K. Lee, D. Yoo, M.F. Rubner, Chem. Mater. 9 (1997) 1710;
(b) F.G. Gao, A. Bard, J. Am. Chem. Soc. 122 (2000) 7426.
[4] (a) Y. Li, Y. Liu, J. Guo, F. Wu, W. Tian, B. Li, Y. Wang, Synth. Met. 118 (2001) 175;
(b) K. Wang, L. Huang, L. Gao, L. Jin, C. Huang, Inorg. Chem. 41 (2002) 3353.
[5] F.G. Gao, A. Bard, J. Chem. Mater. 14 (2002) 3465.
[6] (a) C.-L. Lee, K.B. Lee, J.-J. Kim, Appl. Phys. Lett. 77 (2000) 2280;
(b) R.R. Das, C.-L. Lee, J.-J. Kim, Mater. Res. Soc. Symp. Proc. 708 (2002), BB3.39.1;
(c) J.P.J. Markham, S.-C. Lo, S.W. Magennis, P.L. Burn, I.D.W. Samuel, Appl. Phys. Lett. 80 (2002) 2645.
[7] (a) S. Lamansky, P. Djurovich, D. Murphy, F. Abdel-Razzaq, H.-F. Lee, C. Adachi, P.E. Burrows, S.R. Forrest, M.E. Thompson, J. Am. Chem. Soc. 123 (2001) 4304;
(b) M.E. Thompson, S. Lamansky, P. Djurovich, D. Murphy, F. Abdel-Razzaq, R. Kwong, S.R. Forrest, M.A. Baldo, P.E. Burrows, US Patent 20020034656A1.
[8] J. Brooks, Y. Babayan, S. Lamansky, P.I. Djurovich, I. Tsyba, R. Bau, M.E. Thompson, Inorg. Chem. 41 (2002) 3055.
[9] V.V. Grushin, N. Herron, D.D. LeCloux, W.J. Marshall, V.A. Petrov, Y. Wang, Chem. Commun. (2001) 1494.
[10] A. Brembilla, D. Roizard, P. Lochon, Syn. Commun. 20 (1990) 3379.
[11] Y. Zhang, C.D. Baer, C.C. Neto, P. O'Brien, D.A. Sweigart, Inorg. Chem. 30 (1991) 1685.
[12] M. Maestri, D. Sandrini, V. Blazani, U. Maeder, A. vonZelewsky, Inorg. Chem. 26 (1987) 1323.
[13] M.G. Colombo, A. Hauser, H.U. Güdel, Inorg. Chem. 32 (1993) 3088.
[14] S. Lamansky, P. Djurovich, D. Murphy, F. Abdel-Razzaq, R. Kwong, I. Tsyba, M. Bortz, B. Mui, R. Bau, M.E. Thompson, Inorg. Chem. 40 (2001) 1704.
[15] I.R. Laskar, T.-M. Chen, Chem. Mater. 16 (2004) 111.
[16] J. Vicente, A. Arcas, D. Bautista, M.C.R. de Arellano, J. Organomet. Chem. 663 (2002) 164.
[17] F.H. Allen, J.E. Davies, J.J. Galloy, O. Johnson, O. Kennard, C.F. Macrae, E.M. Mitchell, G.F. Mitchell, J.M. Smith, D.G. Watson, J. Chem. Inf. Comput. Sci. 31 (1991) 187.
[18] F.O. Garces, K. Dedian, N.L. Keder, R. Watts, J. Acta Crystallogr. C 49 (1993) 1117.
[19] R. Urban, R. Krämer, S. Mihan, K. Polborn, B. Wagner, W. Beck, J. Organomet. Chem. (2000) 1039.
[20] F. Neve, A. Crispini, Eur. J. Inorg. Chem. (2000) 1039.
[21] K.A. King, P.J. Spellane, R.J. Watts, J. Am. Chem. Soc. (1985) 1431.
[22] J.N. Demas, G.A. Crosby, J. Phys. Chem. (1971) 991.